Supplement of Biogeosciences, 21, 5027–5043, 2024
https://doi.org/10.5194/bg-21-5027-2024-supplement

Biogeosciences Open Access EGU

Supplement of

Distinct impacts of the El Niño–Southern Oscillation and Indian Ocean Dipole on China's gross primary production

Ran Yan et al.

Correspondence to: Jun Wang (wangjun@nju.edu.cn) and Weimin Ju (juweimin@nju.edu.cn)

Method

Building on the methodology introduced by Ahlstrom et al. [2015], we incorporate an index that evaluates individual geographic locations based on their consistency, over time, in mirroring the sign and magnitude of the national GPP. For each geographical division *j*, its contribution to the national GPP anomaly is defined as:

$$f_j = \frac{\sum_t \frac{x_{jt}|X_t|}{X_t}}{\sum_t |X_t|}$$

where x_{jt} is the GPP anomaly for region *j* at season *t* (SON(y0), DJF(y0), MAM(y1) and JJA(y1)), and X_t is the national GPP anomaly, such that $X_t = \sum_t x_{jt}$. By this definition f_j is the average relative anomaly x_{jt}/X_t for region *j*, weighted with the absolute national anomaly $|X_t|$.

Table S1. Information for the 7 sites used for verification. Where, P represents average annual precipitation, T represents average annual temperature, and PFT represents plant functional types.

Site Name	Lat (°N)	Lon (°E)	P (mm)	T (°C)	PFT	years
Xishuangbanna (BN)	21.93	101.27	737.1	19.40	Forest	2003~2010
Qianyanzhou (QYZ)	26.74	115.06	583.70	17.74	Forest	2003~2010
Changbaishan (CB)	42.40	128.10	234.33	3.65	Forest	2003~2010
Dinghushan (DHS)	23.17	112.53	729.09	20.12	Forest	2003~2010
Haibei Shrub (HBS)	37.67	101.33	236.33	−1.26	Shrub	2003~2010
Dangxiong (DX)	30.50	91.07	220.85	2.72	Grass	2004~2010
Yingke (YK)	38.85	100.42	31.71	7.40	Crop	2008~2010

Table S2. Contributions of different regions to the national GPP changes in different events.

	Southern	Northern	Northwest	TP
El Niño	59.58%	27.29%	4.47%	8.66%
La Niña	76.21%	27.96%	0.46%	−4.64%
pIOD	53.65%	31.67%	6.88%	7.79%
nIOD	37.25%	46.99%	7.48%	8.28%

Table S3. Total GPP anomaly (Tg C yr^{-1}) at the provincial scale for different events. The province names are abbreviated and sorted alphabetically.

Province	El Niño	La Niña	pIOD	nIOD
Anhui	−2.25	4.41	−1.72	3.39
Beijing	0.16	−0.15	0.09	−0.21
Chongqing	2.31	−0.03	0.58	−0.58
Fujian	−0.49	1.62	−22.00	5.36
Gansu	0.05	−0.33	4.00	−3.36
Guangdong	4.17	−2.30	−19.58	2.80
Guangxi	0.05	−2.31	−23.22	−0.33
Guizhou	−2.05	0.94	−6.42	−0.55
Hannan	−0.64	0.87	−6.62	2.18
Hebei	−2.98	0.24	4.62	−1.64
Henan	0.17	2.62	12.80	2.53
Heilongjiang	1.54	−5.13	11.18	−1.18
Hubei	−0.99	−0.15	−12.83	2.76
Hunan	1.23	0.70	−1.72	0.45
Jilin	−0.31	0.36	−0.97	−1.54
Jiangsu	−2.64	1.71	2.77	−0.54
Jiangxi	−2.24	2.24	−32.74	4.31
Liaoning	−2.27	3.67	−3.47	−2.18
Inner Mongolia	−5.77	6.29	−5.97	−12.18
Ningxia	0.08	−0.01	0.11	−0.43
Qinghai	0.21	−0.80	−2.02	−2.96
Shandong	−3.68	1.67	6.37	1.12
Shanxi	1.05	1.86	7.85	−1.69
Shaanxi	5.48	−0.85	10.05	−2.63
Sichuan	−4.22	−2.45	7.14	−3.34
Taiwan	−0.47	0.66	−1.18	0.65
Tianjin	−0.23	−0.09	−0.18	−0.13
Tibet	−2.50	−1.31	6.13	3.05
Xinjiang	3.82	−4.37	−1.46	2.25
Yunnan	−22.55	3.62	−28.20	12.04
Zhejiang	−0.84	1.05	−2.91	1.62

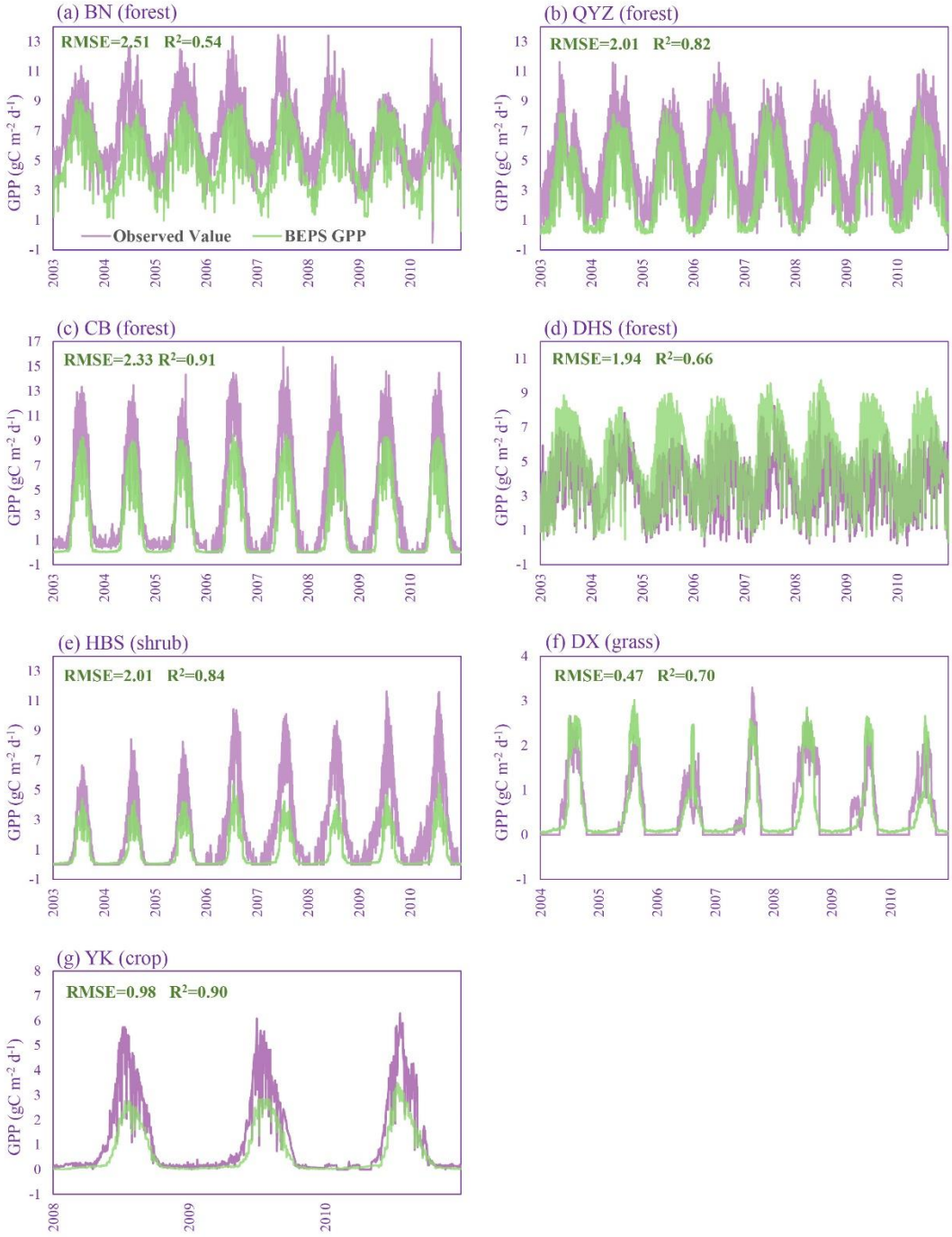

Fig. S1. Comparison between BEPS simulated and Flux Tower observed daily GPP at 7 sites.

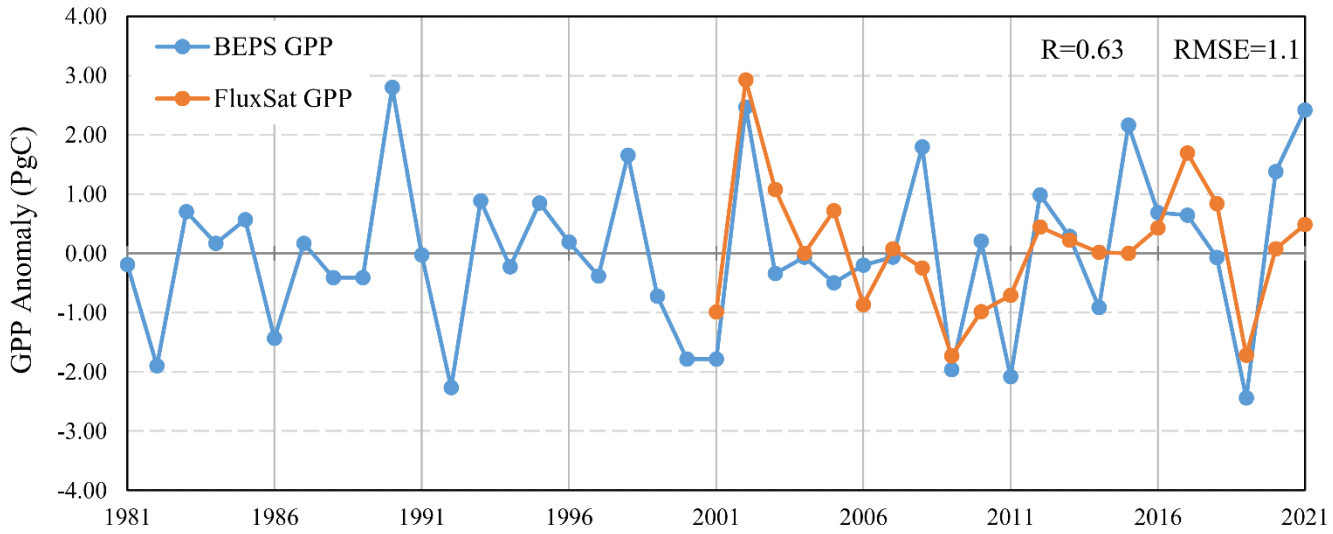

Fig. S2. Total annual gross primary productivity (GPP) anomalies in the Boreal Ecosystem Productivity Simulator (BEPS) model and FluxSat data from 1981 to 2021.

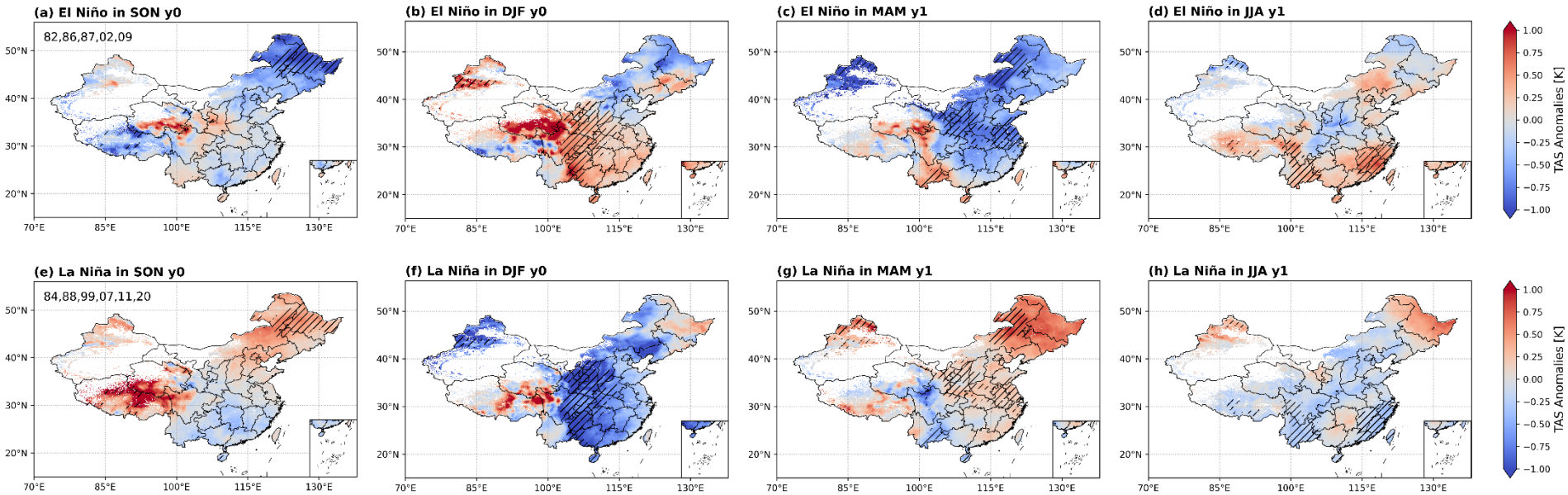

Fig. S3. Spatial distributions of seasonal composite surface air temperature (TAS) anomalies for ENSO events. The black slashes indicate areas where El Niño events differ significantly from La Niña events ($p \leq 0.05$) based on the Student's two−sample *t*-test. Numbers in subplots (first column) denote the years for composite analysis.

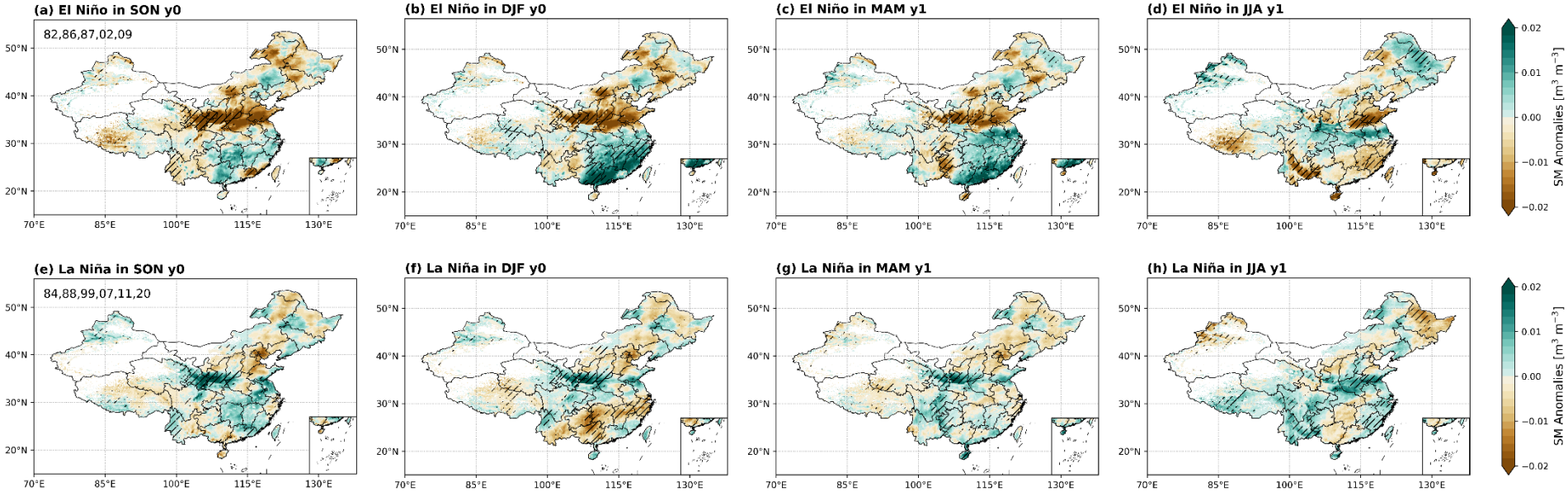

Fig. S4. Same as Fig. S2, but for soil moisture (SM).

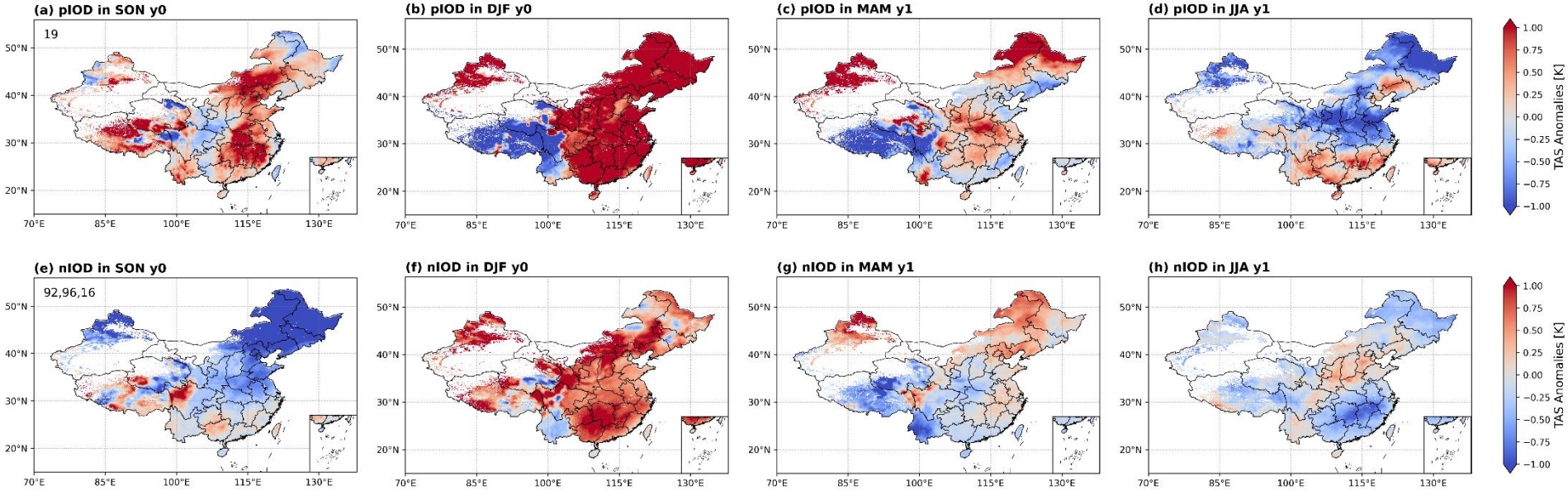

Fig. S5. Spatial distributions of seasonal composite TAS anomalies for IOD events. Numbers in subplots (first column) denote the years for composite analysis.

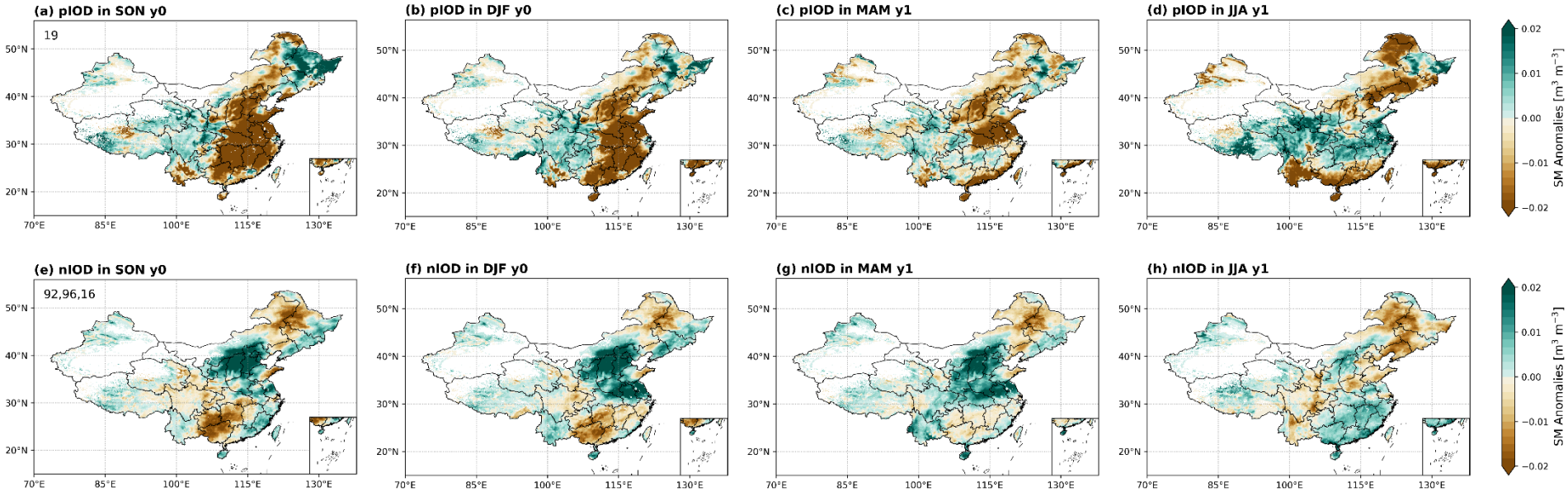

Fig. S6. Same as Fig. S4, but for SM.

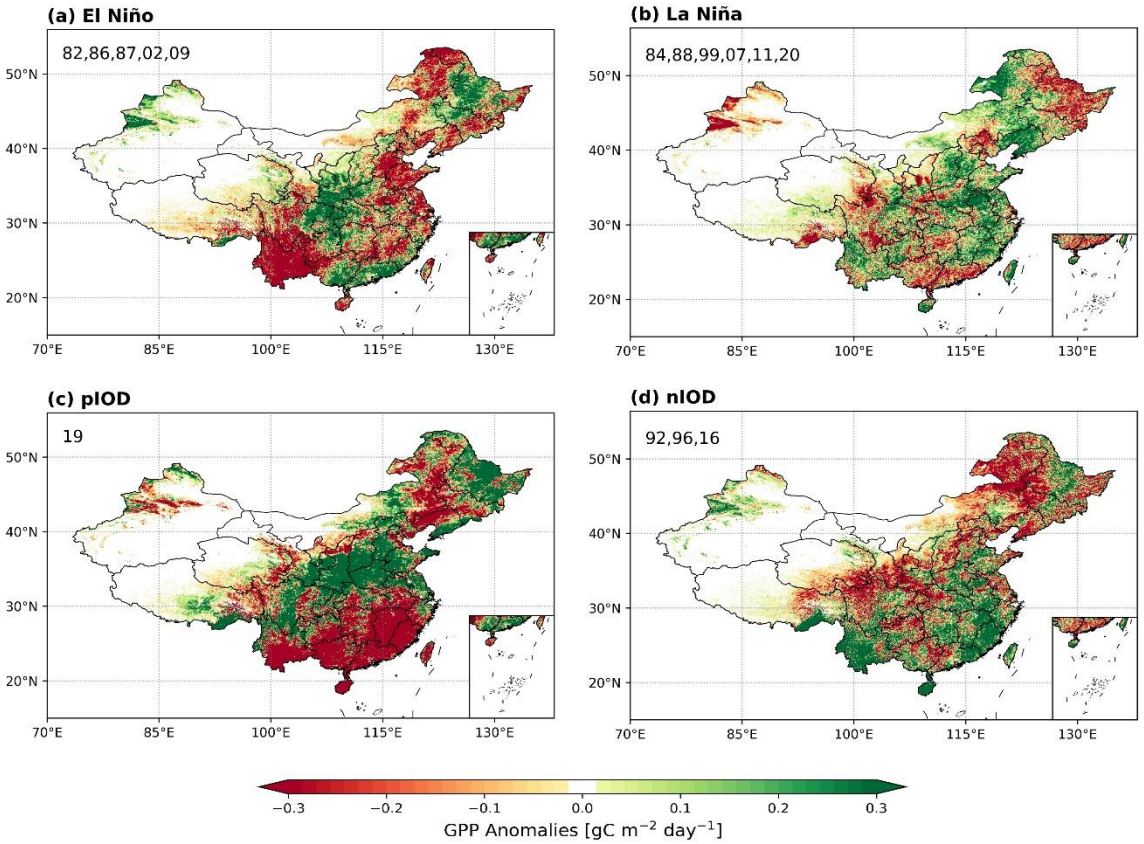

Fig. S7. Spatial distributions of annual total composite GPP anomalies for different event classes. Numbers in subplots denote the years for composite analysis.

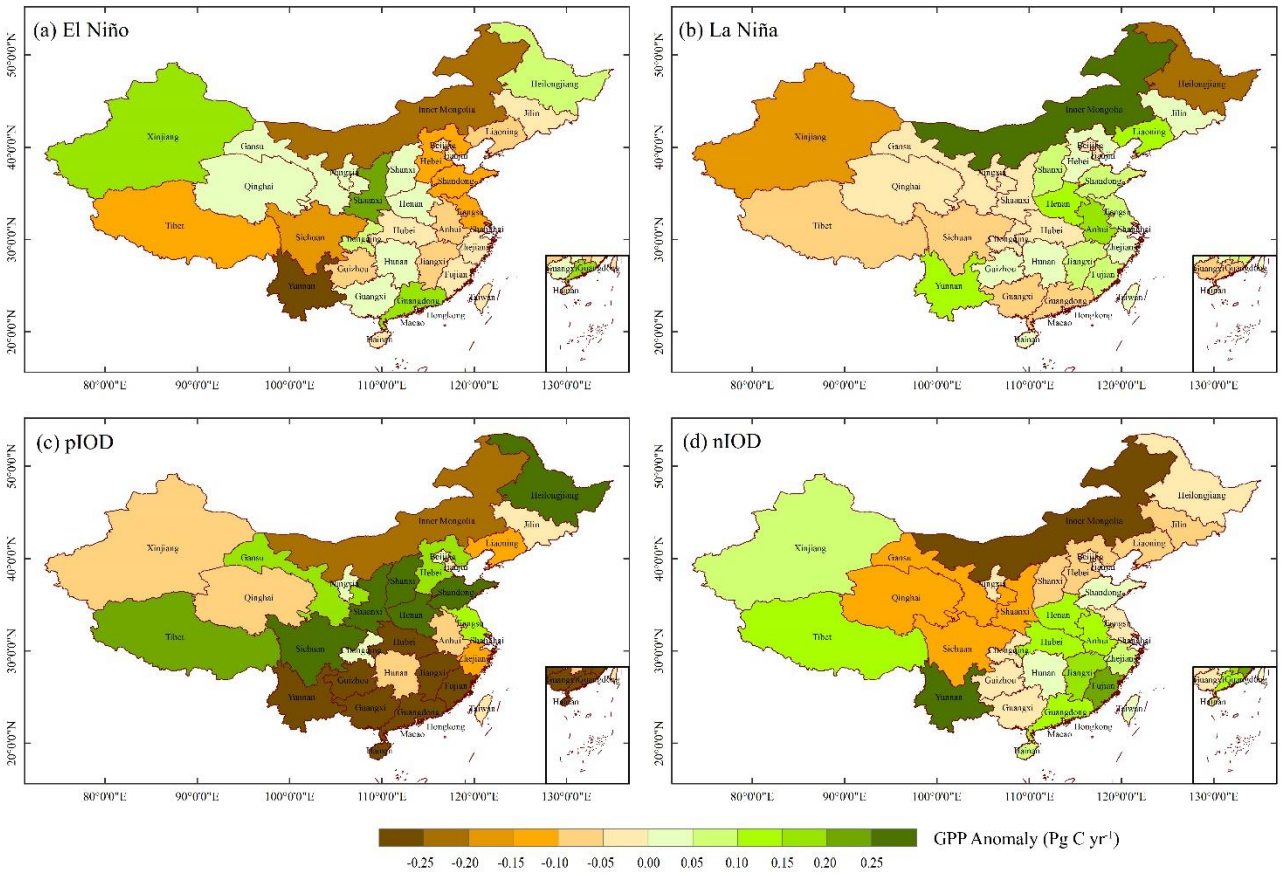

Fig. S8. Spatial distributions of total composite GPP anomalies (Pg C yr^{-1}) at the provincial scale for different classified events.

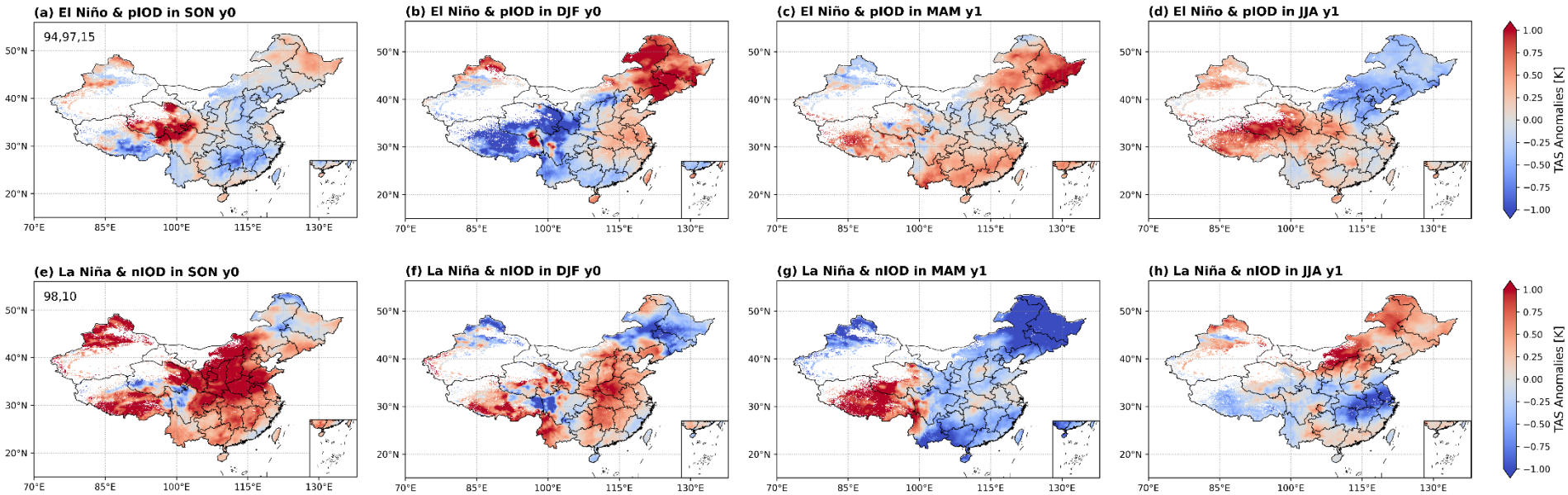

Fig. S9. Spatial distributions of seasonal composite TAS anomalies for compound events. Numbers in subplots (first column) denote the years for composite analysis.

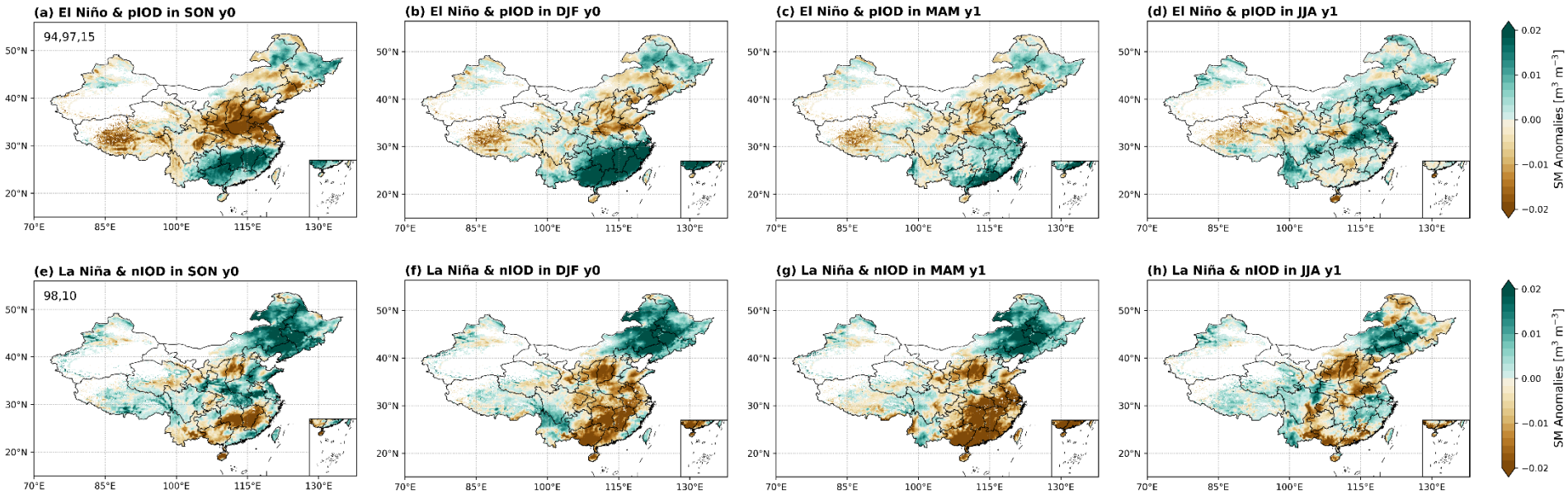

Fig. S10. Same as Fig. S8, but for SM.

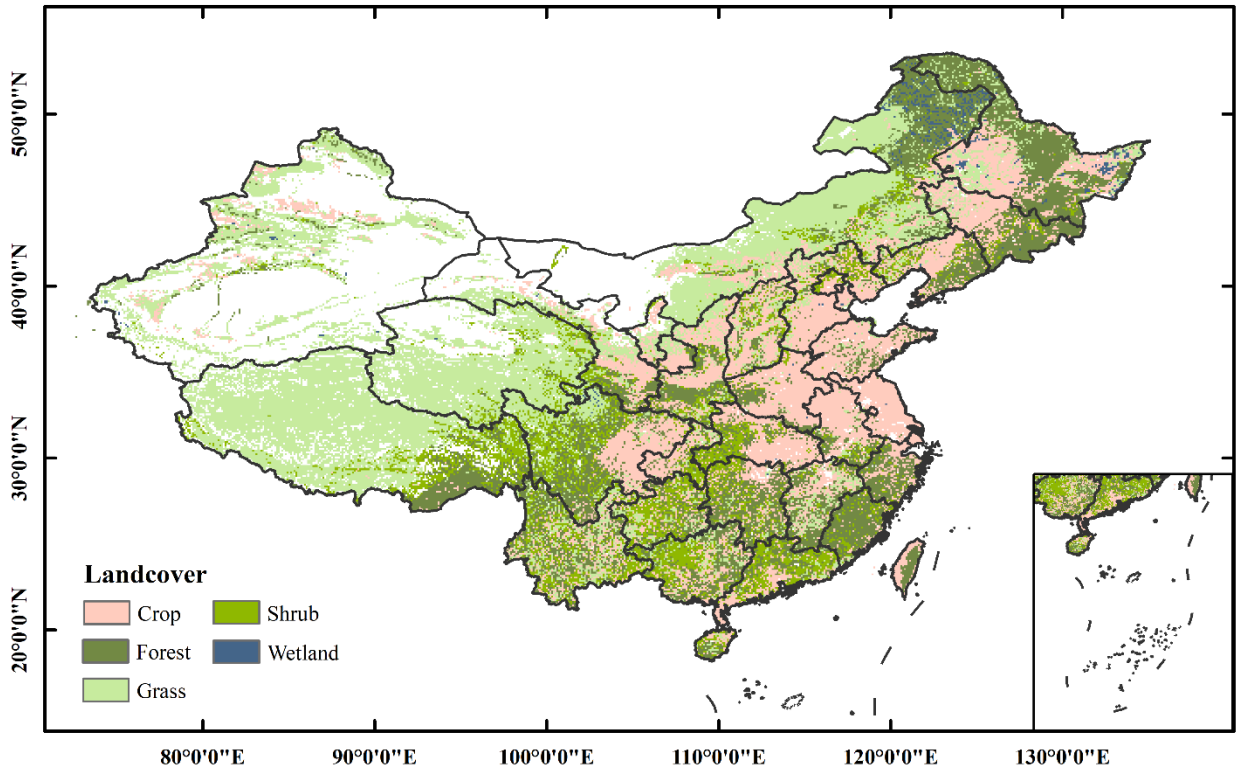

Fig. S11. Geographical distributions of landcover classes, based on the 1:1 000 000 Atlas of vegetation in China (https://www.resdc.cn/data.aspx?DATAID=122). In this study, the data were resampled to 0.1°×0.1° using the area maximization method. Specifically, forest contains its needleleaf forests, broadleaf forests and mixed forests; grass contains grassland, grass, and meadow; crop refers to cultivated vegetation, including crops and artificial orchards and economic forests.

Reference

Ahlstrom, A., et al. (2015), The dominant role of semi-arid ecosystems in the trend and variability of the land CO2 sink, Science, 348(6237), 895-899, https://doi:10.1126/science.aaa1668.